Full-spectrum phonon relaxation times in crystalline Si from molecular dynamics simulations

Hong Zhao[1,a] and Jonathan B. Freund[2]
[1]*Department of Mechanical Science and Engineering, University of Illinois at Urbana-Champaign, Urbana, Illinois 61801, USA*
[2]*Department of Mechanical Science and Engineering, University of Illinois at Urbana-Champaign, Urbana, Illinois 61801, USA and Department of Aerospace Engineering, University of Illinois at Urbana-Champaign, Urbana, Illinois 61801, USA*

(Received 31 October 2007; accepted 2 June 2008; published online 4 August 2008)

The lattice vibrations of a periodic silicon crystal are simulated by a molecular dynamics simulation. The history of atomic displacements and velocities obtained is used to compute the amplitudes of all phonon modes supported by the lattice. The phonon amplitude autocorrelation coefficients are found to decay exponentially in time, in agreement with single-mode relaxation time models for phonon scattering. However, the relaxation times extracted from the correlation curves are found to differ significantly from the empirical formulas currently used in models for microscale thermal transport, suggesting that improved relaxation time models are needed for accurate predictions in complex small-scale heat transfer systems. © *2008 American Institute of Physics*. [DOI: 10.1063/1.2963721]

I. INTRODUCTION

The phonon Boltzmann transport equation[1] (BTE) is a semiclassical model for studying and modeling thermal transport in materials in which phonons are the dominant thermal energy carriers. It is particularly useful at length scales comparable to the phonon mean free path, where ballistic transport causes the Fourier diffusion law to fail. In essence, the BTE constitutes a balance between phonon scattering and net phonon fluxes caused by a temperature gradient. A phonon mode, designated by its wave number $\mathbf{q}$ and polarization index s, satisfies the transport equation

$$\frac{\partial n_s(\mathbf{q};\mathbf{x},t)}{\partial t} + \mathbf{c}_s(\mathbf{q}) \cdot \nabla T(\mathbf{x},t) \frac{\partial n_s(\mathbf{q};\mathbf{x},t)}{\partial T} = \left. \frac{\partial n_s(\mathbf{q};\mathbf{x},t)}{\partial t} \right|_{\text{scatt}}, \tag{1}$$

where $n_s(\mathbf{q};\mathbf{x},t)$ is the local phonon number density, $\mathbf{c}_s(\mathbf{q})$ is the phonon group velocity, T is the local temperature, and the right-hand side is the phonon scattering rate due to multiphonon processes, defects, and impurities.

For numerical solution, the phonon frequency and group velocity in Eq. (1) can be easily computed from the harmonic phonon dispersion relation, but the scattering is more difficult to represent, especially the anharmonic scattering term due to multiphonon processes. In principle, anharmonic scattering can be expressed as the sum of convolutions representing three- and four-phonon interactions, and the discrete BTE resulted can be solved either approximately by a variational principle[2] or numerically exactly through iteration.[3] For example, the lattice thermal conductivity of a cubic silicon carbide crystal computed by this approach is in excellent agreement with experiments at all temperatures measured.[3] However, because of the cost of computing the convolutions, this direct approach seems limited to small effectively one-dimensional systems with uniform temperature gradients.

For larger or complex systems, the phonon relaxation time model is widely used to simplify the computation of the phonon scattering term. In the single-mode relaxation time model, the scattering term has the simple form[4]

$$\left. \frac{\partial n}{\partial t} \right|_{\text{scatt}} = \frac{n^{\text{eq}} - n}{\tau}, \tag{2}$$

where n^{eq} is the phonon density at thermal equilibrium and τ is the phonon relaxation time. The overall phonon scattering rate is proportional to τ^{-1}, which can be viewed as the sum of contributions from anharmonicity, boundary scattering, and impurities,

$$\tau^{-1} = \tau_{\text{anharm}}^{-1} + \tau_b^{-1} + \tau_{\text{imp}}^{-1}. \tag{3}$$

The mechanism of the boundary and impurity scatterings is well understood, and their scattering rates, τ_b^{-1} and τ_{imp}^{-1}, can be computed rigorously.[5–7] The anharmonic scattering rate, $\tau_{\text{anharm}}^{-1}$, is more difficult to determine and is the subject of our investigation. In the simplest "gray" BTE model,[8,9] all phonon modes share the same τ_{anharm} (or more simply the same τ), which is chosen such that the overall lattice thermal conductivity matches that by experiments. Improved models have τ_{anharm} as a function of the temperature, phonon frequency, and polarizations.[10,11] These τ have assumed (often *ad hoc*) functional forms whose coefficients are selected to fit experimental thermal conductivities.[5,6,12] The isotropic $\omega \propto \|\mathbf{q}\|$ Debye model[13] is typically used in both the data fitting for τ and the subsequent solution of the BTE model using the fitted τ. This isotropy assumption, however, weakens at high temperatures where the contribution to thermal conductivity from high-frequency phonons is significant. Relaxation time models can be extremely sensitive to the assumed functional forms for τ: different forms can lead to the fitted scattering rates of longitudinal phonon modes that differ by a factor 10.[6,14] Thus, even though these relaxation time models can

[a]Electronic mail: hongzhao@uiuc.edu.

reproduce the overall thermal conductivity, it remains uncertain whether the predicted phonon distributions are reliable.

In this work, we focus on a direct computation of τ_{anharm} for crystalline silicon. We compute the phonon amplitudes from the atomic displacements and velocities obtained from a molecular dynamics simulation. The structural coherence of a phonon is lost in time because of scattering, which manifests itself as a decay of the autocorrelation coefficients for the phonon amplitude. This decay is seen to be exponential, so mode dependent relaxation times are extracted from the decaying rates by linear regressions. Similar approaches were used by McGaughey and Kaviany[15] to compute the phonon relaxation times in fcc lattices and by Henry and Chen[27] for Si crystal. An important improvement made in this study is that the complex phonon amplitude instead of the normal mode energy as defined in those previous studies is used for computing the autocorrelations, where the phonon amplitude is roughly proportional to the square root of the normal mode energy. In the context of the classical molecular dynamics simulations, the anharmonic phonon-phonon interactions cause not only time variation in the amplitudes of normal modes but also the drift of their phase angles; both factors are captured here by the usage of the complex phonon amplitude. The method is detailed in Sec. II, and the numerical results are compared directly with existing empirical models in Sec. III.

II. METHODS

A. Molecular dynamics simulations

A silicon crystal has a composite face-centered-cubic (fcc) lattice structure, with each fcc site associated with two atoms equilibrated at $\mathbf{R}=(l/2,m/2,n/2)a$ and $\mathbf{R}+(\frac{1}{4},\frac{1}{4},\frac{1}{4})a$, where a is the cubic unit cell width and (l,m,n) is an integer triplet with $l+m+n$ being even. The simulated periodic lattice has $8\times8\times8$ conventional cubic cells, each of which consists of four fcc sites, and so there are 4096 atoms in the lattice. The overall thermal conductivity computed via a Green–Kubo formulation for this system size has been shown to be within 5% of the limiting value for large systems.[16]

The target temperature of the simulation is 800 K, and the lattice constant a is set to be 5.442 Å to account for thermal expansion.[17,18] Interatomic forces are computed using the Stillinger–Weber potential,[19] which has been shown to yield accurate thermal conductivities in the past.[16,20] The numerical time step is $\Delta t=0.5$ fs, which is about one-hundredth of the shortest phonon period (about 50 fs).[21] In the first 10^4 time steps, a Berendson thermostat[22] is applied to bring the temperature to 800 K. The system then evolves as a microcanonical system for another 0.5 ns, which is more than five times the longest relaxation times we report. Thereafter, the system is considered to be in thermal equilibrium, and the atomic displacements and velocities are stored every five time steps for the next 14×10^6 steps needed for our analysis.

B. Phonon dispersion

The same approach as in our phonon interface reflection study[21] is used here to compute phonon dispersion. The Stillinger–Weber potential has a small displacement expansion,

$$U=\frac{1}{2}\sum_{\mathbf{R},\mathbf{R}'}\mathbf{u}^T(\mathbf{R})\mathbf{D}(\mathbf{R}'-\mathbf{R})\mathbf{u}(\mathbf{R}')+O(\|\mathbf{u}\|^3), \tag{4}$$

where $\mathbf{R}$ and $\mathbf{R}'$ are the positions of the fcc lattice sites at equilibrium, $\mathbf{u}(\mathbf{R})$ is the atomic displacement at $\mathbf{R}$, and $\mathbf{D}(\mathbf{R}'-\mathbf{R})$ is the interaction matrix between atoms at $\mathbf{R}$ and $\mathbf{R}'$. Because of the composite fcc lattice structure, each vector $\mathbf{u}$ has six elements and $\mathbf{D}$ is a 6×6 matrix. The elements of $\mathbf{D}$, which are the second-order derivatives of U with respect to atomic displacements about the equilibrium, are computed by adaptive numerical differentiation,[23] with the error in each matrix element being less than $10^{-8}\|\mathbf{D}\|_\infty$.

For a phonon mode of wave number $\mathbf{q}$, its frequency ω and polarization vector $\boldsymbol{\xi}$ are determined from the eigenvalue problem

$$M\omega^2\boldsymbol{\xi}=\hat{\mathbf{D}}(\mathbf{q})\boldsymbol{\xi}, \tag{5}$$

where M is the atomic mass and $\hat{\mathbf{D}}$ is a dynamical matrix,

$$\hat{\mathbf{D}}(\mathbf{q})=\sum_{\mathbf{R}}\mathbf{D}(\mathbf{R})\exp(i\mathbf{q}\cdot\mathbf{R}). \tag{6}$$

Since $\hat{\mathbf{D}}$ is Hermitian, Eq. (5) has six non-negative eigenvalue solutions ω_s^2 $(s=1,2,\ldots,6)$ with orthonormal polarization vectors,

$$\boldsymbol{\xi}_{s_1}^H(\mathbf{q})\boldsymbol{\xi}_{s_2}(\mathbf{q})=\delta_{s_1s_2}, \tag{7}$$

where the superscript H denotes a conjugate transpose. It can be easily shown that two corresponding phonon modes with opposite wave numbers satisfy symmetry conditions

$$\omega_s(-\mathbf{q})=\omega_s(\mathbf{q}) \quad \text{and} \quad \boldsymbol{\xi}_s(-\mathbf{q})=\boldsymbol{\xi}_s^*(\mathbf{q}). \tag{8}$$

To determine the phonon group velocity, which is needed for computing the contribution to thermal conductivity from each phonon mode, we decompose $\hat{\mathbf{D}}$ as

$$\hat{\mathbf{D}}(\mathbf{q})=\exp\left(-\frac{iq_xa}{2}\right)\hat{\mathbf{D}}_L+\hat{\mathbf{D}}_C+\exp\left(\frac{iq_xa}{2}\right)\hat{\mathbf{D}}_R, \tag{9}$$

where $\hat{\mathbf{D}}_L$, $\hat{\mathbf{D}}_C$, and $\hat{\mathbf{D}}_R$ represent a fcc lattice site's interactions with the atoms to its left, in the same y-z plane, and to its right, respectively. The x-component of the group velocity can then be computed as

$$c_x=\frac{\partial\omega}{\partial q_x}=-\operatorname{Im}\left[\frac{a}{2M\omega}\exp\left(\frac{iq_xa}{2}\right)\boldsymbol{\xi}^H\hat{\mathbf{D}}_R\boldsymbol{\xi}\right]. \tag{10}$$

C. Phonon mode decomposition

Any periodic vector function defined on the lattice, which we denote by $\mathbf{f}$, has Fourier decomposition,

$$\mathbf{f}(\mathbf{R}) = \frac{1}{\sqrt{N}} \sum_{\mathbf{q},s} \hat{f}_s(\mathbf{q}) \boldsymbol{\xi}_s(\mathbf{q}) \exp(i\mathbf{q}\cdot\mathbf{R}), \tag{11}$$

where $\mathbf{R}$ is any fcc lattice site, $\mathbf{q}$ denotes a phonon wave number consistent with the periodic boundary condition, s is the phonon branch, and N is the number of fcc lattice sites. The Fourier component $\hat{f}_s$ in Eq. (11) is determined by an inverse transform,

$$\hat{f}_s(\mathbf{q}) = \frac{1}{\sqrt{N}} \sum_{\mathbf{R}} \boldsymbol{\xi}_s^H(\mathbf{q}) \mathbf{f}(\mathbf{R}) \exp(-i\mathbf{q}\cdot\mathbf{R}). \tag{12}$$

Conventionally, the phonon wave numbers are defined within the first Brillouin zone of the reciprocal lattice,

$$-\frac{2\pi}{a} \leqslant q_x, q_y, q_z < \frac{2\pi}{a} \quad \text{and} \quad |q_x| + |q_y| + |q_z| \leqslant \frac{3\pi}{a}. \tag{13}$$

To use a fast Fourier transform algorithm to compute $\hat{f}$, we equivalently define $\mathbf{q}$ in a rectangular unit cell so that

$$0 \leqslant q_x < \frac{2\pi}{a}, \quad -\frac{2\pi}{a} \leqslant q_y < \frac{2\pi}{a}, \quad -\frac{2\pi}{a} \leqslant q_z < \frac{2\pi}{a}, \tag{14}$$

and so the wave numbers supported are

$$q_x = \frac{2\pi}{a}\frac{n_x}{N_x}, \quad n_x = 0, 1, \ldots, N_x - 1, \tag{15a}$$

$$q_y = \frac{2\pi}{a}\frac{n_y}{N_y}, \quad n_y = -N_y, -N_y + 1, \ldots, N_y - 1, \tag{15b}$$

$$q_z = \frac{2\pi}{a}\frac{n_z}{N_z}, \quad n_y = -N_z, -N_z + 1, \ldots, N_z - 1. \tag{15c}$$

Applying this to the lattice vibration, the atomic displacement $\mathbf{u}$ and velocity $\mathbf{v}$ have Fourier decompositions

$$\mathbf{u}(\mathbf{R},t) = \frac{1}{\sqrt{N}} \sum_{\mathbf{q},s} \hat{u}_s(\mathbf{q},t) \boldsymbol{\xi}_s(\mathbf{q}) \exp(i\mathbf{q}\cdot\mathbf{R}), \tag{16a}$$

$$\mathbf{v}(\mathbf{R},t) = \frac{1}{\sqrt{N}} \sum_{\mathbf{q},s} \hat{v}_s(\mathbf{q},t) \boldsymbol{\xi}_s(\mathbf{q}) \exp(i\mathbf{q}\cdot\mathbf{R}). \tag{16b}$$

From Eq. (8), the Fourier coefficients satisfy

$$\hat{u}_s(-\mathbf{q},t) = \hat{u}_s^*(\mathbf{q},t) \quad \text{and} \quad \hat{v}_s(-\mathbf{q},t) = \hat{v}_s^*(\mathbf{q},t). \tag{17}$$

If the lattice potential energy were purely harmonic, the lattice vibration would be the linear superposition of all possible vibrational modes,

$$\mathbf{u}(\mathbf{R},t) = \mathrm{Re}\left[\frac{1}{\sqrt{N}} \sum_{\mathbf{q},s} \phi_s(\mathbf{q},t) \boldsymbol{\xi}_s(\mathbf{q}) \exp(i\mathbf{q}\cdot\mathbf{R}) \right]. \tag{18}$$

where each vibrational mode evolves independently as a harmonic oscillator with amplitude

$$\phi_s(\mathbf{q},t) = \phi_s(\mathbf{q},0) \exp[-i\omega_s(\mathbf{q})t]. \tag{19}$$

Those amplitudes can be computed from $\hat{u}$ and $\hat{v}$ as follows. Using Eq. (8), we can recraft Eq. (18) as

$$\mathbf{u}(\mathbf{R},t) = \frac{1}{\sqrt{N}} \sum_{\mathbf{q},s} \frac{1}{2}[\phi_s(\mathbf{q},t) + \phi_s^*(-\mathbf{q},t)] \boldsymbol{\xi}_s(\mathbf{q}) \exp(i\mathbf{q}\cdot\mathbf{R}), \tag{20}$$

which, when compared to Eq. (16a), leads to the relation

$$\tfrac{1}{2}[\phi_s(\mathbf{q},t) + \phi_s^*(-\mathbf{q},t)] = \hat{u}(\mathbf{q},t). \tag{21}$$

Since

$$\frac{d}{dt}\phi_s(\mathbf{q},t) = -i\omega_s(\mathbf{q})\phi_s(\mathbf{q},t), \tag{22}$$

the time derivative of Eq. (18) is

$$\dot{\mathbf{u}}(\mathbf{R},t) = \mathbf{v}(\mathbf{R},t) = \mathrm{Re}\left[\frac{1}{\sqrt{N}} \sum_{\mathbf{q},s} -i\omega_s(\mathbf{q},t)\phi_s(\mathbf{q},t)\boldsymbol{\xi}_s(\mathbf{q}) \exp(i\mathbf{q}\cdot\mathbf{R}) \right]. \tag{23}$$

This, combined with Eq. (16b), gives a second relation that links ϕ and $\hat{v}$,

$$\frac{1}{2}[\phi_s(\mathbf{q},t) - \phi_s^*(-\mathbf{q},t)] = i\frac{\hat{v}_s(\mathbf{q},t)}{\omega_s(\mathbf{q})}. \tag{24}$$

From Eqs. (21) and (24), the phonon amplitudes can be determined by either of the following two equations:

$$\phi_s(\mathbf{q},t) = \hat{u}_s(\mathbf{q},t) + i\frac{\hat{v}_s(\mathbf{q},t)}{\omega_s(\mathbf{q})}, \tag{25a}$$

$$\phi_s(-\mathbf{q},t) = \hat{u}_s^*(\mathbf{q},t) - i\frac{\hat{v}_s^*(\mathbf{q},t)}{\omega_s(\mathbf{q})}. \tag{25b}$$

The compatibility between the two formulations in Eqs. (25a) and (25b) above can be easily shown by using symmetries (8) and (17). While the derivation for ϕ is from a perspective of classical mechanics, it can be easily verified that the correspondence to the quantum formulation is

$$\phi_s(\mathbf{q}) = -i\sqrt{\frac{2\hbar}{M\omega}} a_s^\dagger(\mathbf{q}), \tag{26}$$

where $a^\dagger$ is the phonon creation operator.[4,7]

For the weak anharmonicity of any realistic lattice potential energy model, every $\phi_s(\mathbf{q},t)$ evolves approximately as Eq. (19), only with a phase $\phi_s(\mathbf{q},t)\exp[i\omega_s(\mathbf{q})t]$ that varies with time. Under the assumption that the time scale of this phase drift is large compared to the phonon vibration time period $2\pi/\omega$, Eqs. (25a) and (25b) still holds approximately. Using Eqs. (25a) and (25b), we compute the phonon amplitudes from the atomic displacements and velocities obtained by the molecular dynamics simulation.

Figure 1 shows the real parts of the amplitudes of two phonon modes. Both modes have $(n_x, n_y, n_z) = (2, 3, 4)$, so that

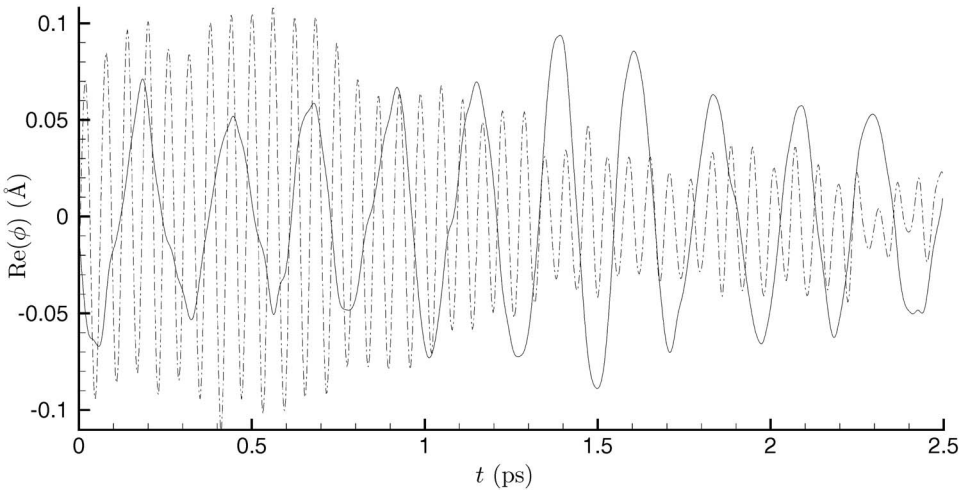

FIG. 1. Phonon amplitude of two modes with $n_x=2$, $n_y=3$, and $n_z=4$ and different branch numbers: (—) $s=1$ and (– - –) $s=6$.

$$\mathbf{q}=\left(\frac{2}{8},\frac{3}{8},\frac{4}{8}\right)\frac{2\pi}{a},$$

and the branch indices are 1 and 6. The time variation of the phonon amplitude is clear in the figure. For every supported phonon mode, we define its anharmonic frequency, ω_{anharm}, as the frequency of the most significant Fourier mode of the amplitude curve. The ratio between this ω_{anharm} and the harmonic frequency ω is plotted in Fig. 2. All anharmonic frequencies are lower than their harmonic counterparts, but within 6% for all phonon modes. The difference between ω and ω_{anharm} is the biggest for phonons with $\omega<50$ ps^{-1}. This agrees well with the experimental results,[24] which show that all silicon phonon frequencies reduce as the temperature and, thus, anharmonic effects increase. In these experiments, the most reduction is observed for transverse acoustic phonons near the boundary point $\mathbf{q}=(2\pi/a,0,0)$ of the Brillouin zone, as we too observe.

Since molecular dynamics simulations of this sort obey Boltzmann statistics, the principle of energy equipartition requires that energy carried by each phonon mode be approximately k_BT. A perfect agreement is only possible in the harmonic limit. The mean energy of a phonon mode can be computed approximately as

$$e_s(\mathbf{q})=\tfrac{1}{2}M\omega_s(\mathbf{q})^2\langle|\phi_s(\mathbf{q},t)|^2\rangle_t, \tag{27}$$

where $\langle|\phi_s(\mathbf{q},t)|^2\rangle_t$ denotes the time average of $|\phi_s(\mathbf{q},t)|^2$. Plotting $e_s(\mathbf{q})/k_BT$ for all phonon modes in Fig. 3 shows that this ratio is between 0.9 and 1.2 for 99% of the modes. Thus, it is in reasonable agreement with the Boltzmann distribution, which supports the use of ϕ to represent phonon amplitudes.

D. Extraction of phonon relaxation times

As traveling waves, phonons in a crystal continually lose their coherence. This can be quantified by the decay of the autocorrelation coefficient of the phonon amplitude,

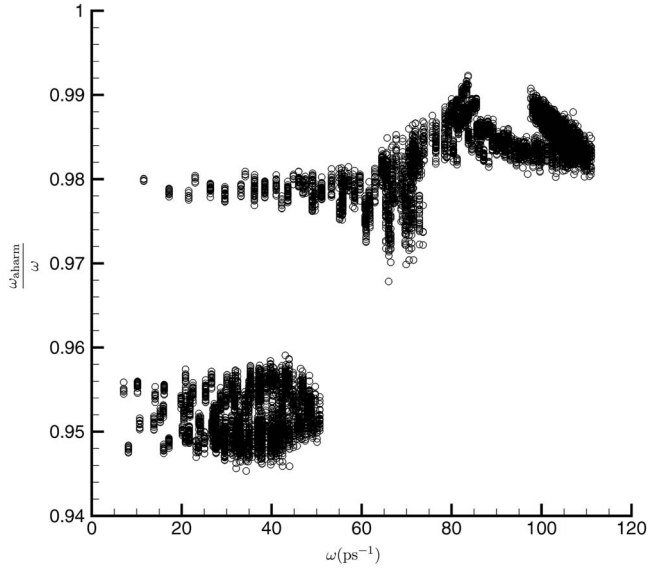

FIG. 2. Comparison between the anharmonic and harmonic phonon frequencies.

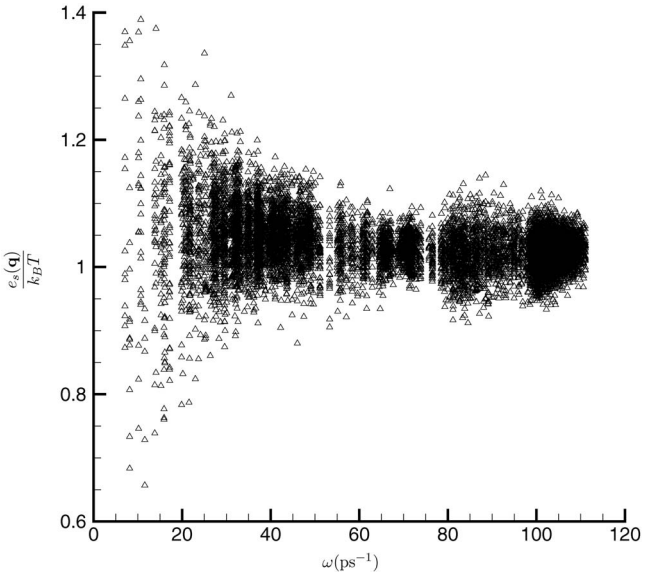

FIG. 3. Phonon energy equipartition for all phonon modes, where $e_s(\mathbf{q})$ as defined in Eq. (27) is the energy carried by the phonon mode of wave number $\mathbf{q}$ and branch s.

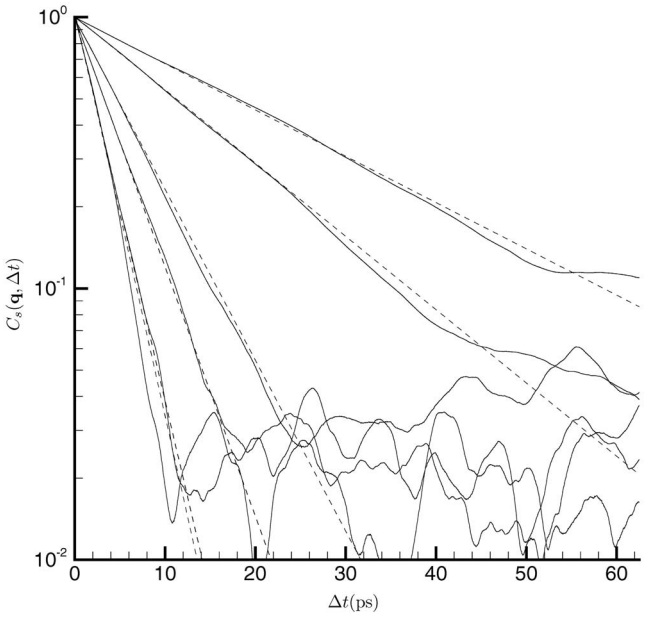

FIG. 4. Phonon amplitude correlation of the six-phonon modes with $n_x=2$, $n_y=3$, and $n_z=4$: — computed as Eq. (28) with exponential fit (---).

$$C_s(\mathbf{q},\Delta t)=\frac{|\langle\phi_s^*(\mathbf{q},t)\phi_s(\mathbf{q},t+\Delta t)\rangle_t|}{\langle|\phi_s(\mathbf{q},t)|^2\rangle_t}. \tag{28}$$

Under the single-mode relaxation time assumptions, $C_s(\mathbf{q},\Delta t)$ decays exponentially with Δt for each phonon mode. Figure 4 shows the plots of the autocorrelation curves of the six-phonon modes with $\mathbf{q}=(1/2,3/4,1)\pi/a$, and they all do indeed decay exponentially. By Eq. (2), the possibility for a phonon to retain its original coherent structure after a time length Δt is $\exp(-\Delta t/\tau)$. Hence the self-correlation in phonon numbers $\langle n(t)n(t+\Delta t)\rangle_t$ also decays as $\exp(-\Delta t/\tau)$. However, the phonon number, as the measure of modal lattice vibration energy [Eq. (27)], is proportional to $|\phi|^2$ in a classical mechanical system, so

$$\frac{d\ln\langle n(t)n(t+\Delta t)\rangle_t}{d\Delta t}=2\frac{d\ln|\langle\phi^*(t)\phi(t+\Delta t)\rangle_t|}{d\Delta t}. \tag{29}$$

We thus compute each time constant $\tau_s(\mathbf{q})$ via

$$\frac{1}{\tau_s(\mathbf{q})}=-2\frac{d\ln C_s(\mathbf{q},\Delta t)}{d\Delta t}, \tag{30}$$

where the right-hand side is by the linear regression of the linear decaying part of the $\ln C_s(\mathbf{q},\Delta t)$ curve, as seen in Fig. 4.

III. RESULTS

The computed phonon relaxation times are plotted in Fig. 5. The relaxation times range from $\sim 10^2$ to ~ 1 ns, and generally decrease with increasing phonon frequencies. Of all phonon modes (including the optical phonons), the shortest relaxation times occur near $\omega=70$ ns^{-1} at the boundary between acoustic and optical modes.

Also plotted in Fig. 5 are the relaxation times of acoustic phonons predicted by Holland[6] and Joshi and Verma,[14] which are typical examples of empirical relaxation time

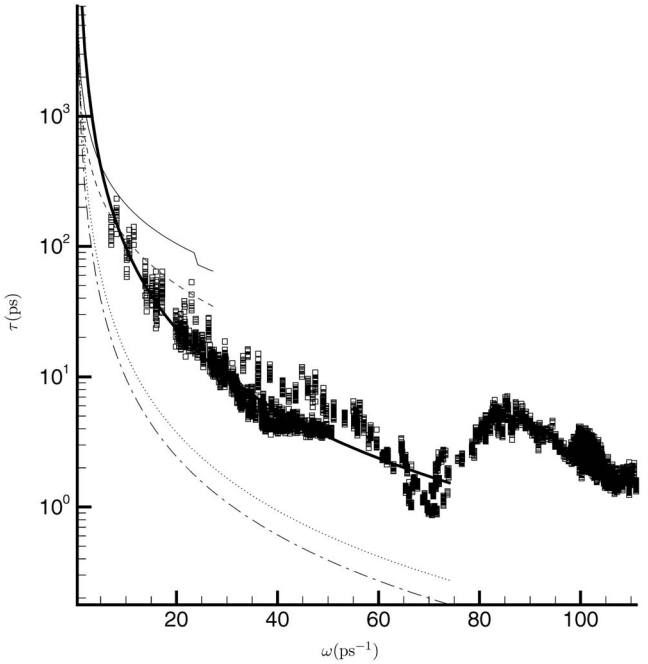

FIG. 5. Phonon relaxation times: Holland (Ref. 6) empirical formula with (—) τ_{TA} and (–·–) τ_{LA}; Joshi and Verma (Ref. 14) empirical formula with (----) τ_{TA} and (·····) τ_{LA}; from the molecular dynamics simulations (□) with the thick solid line showing a power-law fit $\tau=1.17\times10^4\omega^{-2.077}$, with τ in ps and ω in ps^{-1}.

models that are used in current BTE models.[10,11] These models have analytical functional forms for the multiphonon scattering rates, with coefficients obtained by fitting the overall thermal conductivity with experiments. A Debye approximation is used for the phonon dispersion relation, and the longitudinal (LA) and transverse (TA) phonon branches are treated separately in these models. Both these models have $\tau_{TA}>10\tau_{LA}$ in their overlapping frequency ranges. In actual crystalline silicon, the polarization vectors $\boldsymbol{\xi}$ computed by solving Eq. (5) are generally neither parallel or perpendicular to the wave vector $\mathbf{q}$, so few phonon modes are distinctively longitudinal or transverse. It is clear, however, that the range of computed relaxation times is much less than that in these models, with the maximum τ being at most five times the minimum at any frequency. The computed relaxation times are all bounded by the τ_{TA} and τ_{LA} of Holland.[6] Joshi and Verma's model[14] is reported to give a better fit of thermal conductivity at high temperatures; their τ_{TA} curve is closer to our values. However, the τ_{LA} curves of both models are below our minimum relaxation times by almost one order of magnitude. The wide separation between τ_{TA} and τ_{LA} in the empirical models might be, in part, an artifact of the Debye model used in crafting them.

The overall lattice thermal conductivity κ as the sum of contributions from all phonon modes can be computed as[25]

$$\kappa=\frac{k_B}{V}\sum_{\mathbf{q},s}\tau_s(\mathbf{q})|c_x(\mathbf{q},s)|^2, \tag{31}$$

where k_B is the Boltzmann constant and V is the volume of the lattice. The κ computed by Eq. (31) is 66.1 W K^{-1} m^{-1}, 10% of which is contributed by optical phonons. The thermal

conductivity can also be computed by the Green–Kubo formula[16]

$$\kappa = \frac{1}{3k_B T^2 V}\int_0^\infty \langle \mathbf{J}(t+s)\cdot\mathbf{J}(t)\rangle_t ds, \tag{32}$$

where $\mathbf{J}(t)$ is the instantaneous energy flux at time t. During the molecular dynamics simulation, the energy fluxes are also computed, and the thermal conductivity by Eq. (32) is $\kappa=76$ W K^{-1} m^{-1}, which is in good agreement with the experimental value of 78 W K^{-1} m^{-1}.[26]

The fact that the κ value predicted by Eq. (31) is 15% smaller than by (32) is not unexpected given that not all phonon scattering causes thermal resistance. Anharmonic scattering due to N-processes and U-processes are both included in τ^{-1}, while only the latter causes thermal resistance. Therefore, when using τ instead of τ_U in Eq. (31), the phonon scattering rate is overestimated, leading to a lower predicted thermal conductivity. Without explicit accounting for the N-type scattering, similar errors are expected when solving BTE even with exact relaxation times.

IV. CONCLUSIONS

We calculate the amplitudes of all phonon modes supported by a periodic silicon lattice from the atomic displacements and velocities obtained by a molecular dynamics simulation. The anharmonic phonon frequencies agree well with the harmonic frequencies; the phonon energy is found to satisfy the principle of energy equipartition. The autocorrelation coefficients of phonon amplitudes are shown to decay exponentially with time, which is consistent with the single-mode relaxation time assumption. The relaxation times are deduced from the decay rate of the correlation coefficients. The lattice thermal conductivity based on the relaxation times is 15% below those by the Green–Kubo formula and by experiments, which is believed to be due to the inclusion of N-processes in the scattering rate.

The relaxation time models by Holland[6] and by Joshi and Verma[14] predict that the relaxation times of transverse acoustic modes, τ_{TA}, is more than a factor of 10 times greater than τ_{LA} of the longitudinal modes. Much less variation is present in our computed relaxation times, which are bounded by these empirical models. Our results suggest that when the realistic anisotropic phonon dispersion models are used, improved relaxation models are also needed. While a good analytical formula over the whole phonon wave number space seems unlikely, the relaxation times can be computed on a discrete phonon wave number space at different temperatures by methods such as the one presented in this paper.

ACKNOWLEDGMENTS

This research was supported by the National Science Foundation Grant No. CTS-0128365.

[1] C. L. Tien, *Microscale Energy Transfer*, Chemical and Mechanical Engineering (Taylor & Francis, London, 1997).
[2] S. Pettersson, Phys. Rev. B **43**, 9238 (1991).
[3] A. Sparavigna, Phys. Rev. B **66**, 174301 (2002).
[4] N. W. Ashcroft and N. D. Mermin, *Solid State Physics* (Thomson Learning Inc., Florence, KY, 1976).
[5] J. Callaway, Phys. Rev. **113**, 1046 (1959).
[6] M. G. Holland, Phys. Rev. **132**, 2461 (1963).
[7] G. P. Srivastava, *The Physics of Phonons* (Adam Hilger, New York, 1990).
[8] G. Chen, Phys. Rev. B **57**, 14958 (1998).
[9] R. G. Yang and G. Chen, Phys. Rev. B **69**, 195316 (2004).
[10] S. Mazumder and A. Majumdar, J. Heat Transfer **123**, 749 (2001).
[11] S. V. J. Narumanchi, J. Y. Murthy, and C. H. Amon, J. Heat Transfer **126**, 946 (2004).
[12] M. G. Holland, Phys. Rev. **134**, A471 (1964).
[13] P. Debye, Ann. Phys. **39**, 789 (1912).
[14] Y. P. Joshi and G. S. Verma, Phys. Rev. B **1**, 750 (1970).
[15] A. J. H. McGaughey and M. Kaviany, Phys. Rev. B **69**, 094303 (2004).
[16] P. K. Schelling, S. R. Phillpot, and P. Keblinski, Phys. Rev. B **65**, 144306 (2002).
[17] C. A. Swenson, J. Phys. Chem. Ref. Data **12**, 179 (1983).
[18] H. Watanabe, N. Yamada, and M. Okaji, Int. J. Thermophys. **25**, 221 (2004).
[19] F. H. Stillinger and T. A. Weber, Phys. Rev. B **31**, 5262 (1985).
[20] Y. H. Lee, R. Biswas, C. M. Soukoulis, C. Z. Wang, C. T. Chan, and K. M. Ho, Phys. Rev. B **43**, 6573 (1991).
[21] H. Zhao and J. B. Freund, J. Appl. Phys. **97**, 024903 (2005).
[22] H. J. C. Berendsen, J. P. M. Postma, W. F. v. Gunsteren, A. DiNola, and J. R. Haak, J. Chem. Phys. **81**, 3684 (1984).
[23] W. H. Press, S. A. Teukolsky, W. T. Vetterling, B. P. Flannery, and M. Metcalf, *Numerical Recipes in Fortran 90* (Cambridge University Press, Cambridge, England, 1996).
[24] V. V. Brazhkin, S. G. Lyapin, I. A. Trojan, R. N. Voloshin, A. G. Lyapin, and N. N. Mel'nik, JETP Lett. **72**, 195 (2000).
[25] D. A. McQuarrie, *Statistical Mechanics* (Harper & Row, New York, 1973).
[26] W. S. Capinski, H. J. Maris, E. Bauser, I. Silier, M. Asen-Palmer, T. Ruf, M. Cardona, and E. Gmelin, Appl. Phys. Lett. **71**, 2109 (1997).
[27] A. Henry and G. Chen, J. Comput. Theor. Nanosci. **5**, 141 (2008).